J. Dairy Sci. 109:2714–2726
https://doi.org/10.3168/jds.2025-26969
© 2026, The Authors. Published by Elsevier Inc. on behalf of the American Dairy Science Association®.
This is an open access article under the CC BY license (https://creativecommons.org/licenses/by/4.0/).

A data fusion approach unveils the effects of 3-nitrooxypropanol on the rumen fluid and milk metabolomes of lactating Holstein dairy cows

G. Rocchetti,[1] F. Froldi,[1] M. Lapris,[1] M. Moschini,[1] P. Bani,[1] L. Cattaneo,[1]* and E. Trevisi[1,2]
[1]Department of Animal Science, Food and Nutrition (DIANA), Faculty of Agricultural, Food and Environmental Sciences, Università Cattolica del Sacro Cuore, 29122 Piacenza, Italy
[2]Romeo and Enrica Invernizzi Research Center for Sustainable Dairy Production of the Università Cattolica del Sacro Cuore (CREI), 29122 Piacenza, Italy

ABSTRACT

This study used a data fusion approach, combining rumen and milk metabolomic profiling, to investigate the biochemical effects of 3-nitrooxypropanol (3-NOP), an effective methanogenesis inhibitor. A controlled feeding trial was conducted in 2 phases (i.e., summer and fall) with Holstein dairy cows (n = 30/phase) fed a diet supplemented for 9 wk with 60 mg/kg DM of 3-NOP or a placebo. Rumen fluid and milk samples were collected at the end of the experimental phases and analyzed using ultra-HPLC coupled with high-resolution mass spectrometry. Metabolomic profiles from the cows supplemented with 3-NOP and the control group were compared to assess the influence of 3-NOP on rumen fermentation and milk composition. Both 3-NOP and the experimental phase significantly influenced rumen metabolites, whereas no significant differences were observed in the milk metabolome with 3-NOP supplementation. Untargeted metabolomic analysis, supported by supervised and unsupervised multivariate statistics, identified significant alterations in rumen metabolites. Results confirmed that 3-NOP significantly alters rumen fermentation by reducing methanogenesis-related compounds (e.g., methyl-coenzyme M and coenzyme B) and influencing nitrogen and nucleic acid metabolism, indicative of changes in microbial fermentation and protein synthesis. Regarding the milk metabolome, changes in certain discriminant metabolites, such as glycerophospholipids, small peptides, and nucleic acids, reflect alterations in rumen fermentation. Although 3-NOP supplementation induced marked changes in the rumen metabolome, including pathways related to methanogenesis and nitrogen metabolism, these alterations were not reflected in major changes in milk quality or its overall metabolomic profile.

Key words: methanogenesis inhibitor, feedomics, metabolomics, rumen, milk

INTRODUCTION

Methanogenesis, the biological production of methane (CH_4) by archaea, is a significant process in ruminant animals (Khairunisa et al., 2023). This process not only contributes to the global emission of GHG but also represents a substantial loss of dietary energy for the host animal (Min et al., 2020). Consequently, mitigation strategies are increasingly being explored to mitigate CH_4 emissions for both feed efficiency and environmental benefits (Min et al., 2020; Króliczewska et al., 2023).

Among the various approaches explored, methanogenesis inhibitors have gained considerable attention (Beauchemin et al., 2020). One proven inhibitor is 3-nitrooxypropanol (**3-NOP**), a compound specifically targeting the key enzyme methyl-coenzyme M reductase (**MCR**), essential for the final step of CH_4 formation (Yu et al., 2021). This inhibition not only reduces GHG emissions but may also affect rumen fermentation and downstream biofluids such as milk and blood (Yanibada et al., 2020, 2021). Several recent studies have demonstrated that 3-NOP included in ruminant diets can significantly reduce CH_4 emissions (typically by 20% to 40%) without adversely affecting animal health or productivity (Pitta et al., 2022a,b; Kebreab et al., 2023; Moschini et al., 2025). Accordingly, the safety and efficacy of 3-NOP for ruminants for milk production and reproduction have been confirmed by the European Food Safety Authority (EFSA, 2021).

The rumen is a complex and dynamic microbial ecosystem with a delicate balance among various microbial populations, fermentation processes, and metabolic outputs. Introducing methanogenesis inhibitors such as 3-NOP can alter this balance, leading to changes in the microbial community structure and metabolic pathways (Pitta et al., 2022a,b). These alterations could influence fermentation efficiency and nutrient absorption (Liu et al., 2022). Moreover, the effects of 3-NOP could ex-

Received May 21, 2025.
Accepted December 5, 2025.
*Corresponding author: luca.cattaneo@unicatt.it

The list of standard abbreviations for JDS is available at adsa.org/jds-abbreviations-26. Nonstandard abbreviations are available in the Notes.

tend to milk, an important biofluid reflecting metabolic changes and animal health (Yanibada et al., 2021). Milk composition (e.g., fatty acid profile, protein and AA contents, and other bioactive compounds) can be affected by changes in rumen fermentation patterns (Rocchetti et al., 2022). Understanding the influence of 3-NOP on milk composition is essential to gain insight into its role in dairy production systems. In recent years, metabolomics has emerged as a strategic approach for determining chemical composition and quantifying key metabolites in different biological fluids and dairy products as related to various biochemical processes (Yanibada et al., 2021; Suh, 2022; Toral et al., 2023). Despite increasing interest in 3-NOP, comprehensive metabolomic studies, especially those focused on the rumen metabolome, are still lacking. Untargeted metabolomics can help reveal biochemical pathways affected by methanogenesis inhibition and improve understanding of rumen responses (de Almeida et al., 2018). Therefore, although 3-NOP clearly affects methane formation, its broader effects on interactions among microbial domains and on major biochemical pathways remain unclear. Moreover, no studies have combined multiple omics datasets across different biofluids to investigate how CH_4 mitigation strategies influence rumen microbes and their functional enzymes. Knowledge about archaea–bacteria interactions in this context also remains limited (Liu et al., 2021).

Starting from these background conditions, this work used a data fusion approach to evaluate the effects of 3-NOP on both rumen and milk metabolomes in Holstein dairy cows fed a corn silage-based and high-starch diet (~29% DM). In the context of metabolomics and omics technologies, a data fusion approach refers to the integration of metabolomic data obtained from different biological matrices—in our case, rumen fluid and milk—to generate a holistic view of metabolic changes (Becchi et al., 2025). This strategy captures complementary information that cannot be obtained when each matrix is analyzed separately, improving understanding of systemic responses to 3-NOP. We hypothesized that 3-NOP supplementation would modify the rumen metabolomic profile through its modulatory effects on the rumen microbiota, while inducing minimal changes in the milk metabolome, given that 3-NOP effects would be largely confined to the rumen. Untargeted metabolomics on multiple biofluids therefore offers a comprehensive approach to evaluating both the benefits and the possible limitations of using methanogenesis inhibitors such as 3-NOP in dairy production systems.

MATERIALS AND METHODS

This study was approved by the Committee for the Protection and Welfare of Experimental Animals of the Università Cattolica del Sacro Cuore and authorized by the Italian Health Ministry (protocol 355/2022-PR). The study was performed at CERZOO (Research Center for Livestock and Environment, s.r.l., Piacenza, Italy), the experimental farm of the Università Cattolica del Sacro Cuore.

Animal Management and Experimental Design

The study's experimental design and animal management have been described in detail in the companion paper (Moschini et al., 2025). The experiment was carried out in 2 phases, equally structured as longitudinal studies with repeated measurements in a completely randomized design. Phase 1 (**P1**) was carried out from May to August 2022, and phase 2 (**P2**) from September to December 2022. Each phase consisted of a 14-d covariate period at the beginning of the study, followed by a 63-d treatment period and a 14-d washout period. Cows were housed in the same pen in a freestall barn (with mattresses covered with chopped straw), equipped with a Roughage Intake Control system (RIC, Hokofarm Group, the Netherlands) for individual monitoring of feed intake and a GreenFeed system unit (C-Lock Inc., Rapid City, SD) for continuous measurements of enteric CH_4, CO_2, and H_2 emissions. A total of 60 multiparous Holstein cows (30 in each phase) in mid- to late lactation without signs of clinical diseases in at least the last 3 wk before the start of the experiments were enrolled in the study. The DIM and milk yield of cows at enrolment were on average (±SD) 190 ± 72 kg/d and 36.8 ± 7.5 kg/d, respectively, for P1, and 158 ± 74 kg/d and 36.8 ± 4.6 kg/d, respectively, for P2. Three cows were excluded from P2 before the end of the experiment because of lack of persistence of the lactation curve (n = 2) or foot problems (n = 1).

At 0900 h, all cows were ad libitum fed a high-starch diet based on corn silage, and alfalfa hay (52% DM, 51.4% forage, 48.6% concentrate, 15.4% CP, 29.1% starch, 3.3% ether extract, 31.9% NDF), suitable for producing milk for Grana Padano Protected Designation of Origin (PDO) cheese-making, and had free access to water. Full details about diet ingredients and chemical compositions are reported in Moschini et al. (2025). After the initial covariate period, during which all the animals received the same diet, cows were randomly assigned to 1 of 2 groups: (1) the 3-NOP treatment group (n = 28), which received the basal diet supplemented with 600 mg/kg DM of Bovaer10 (dsm-firmenich Animal Nutrition and Health, Kaiseraugst, Switzerland; containing 100 g/kg of 3-NOP on silicon dioxide + 1,2-propanediol) included in a premix; or (2) the control group (**CTR**; n = 29), which received the same diet with a premix containing 600 mg/kg DM of a carrier control containing only silicon dioxide 1,2-propanediol. The 3-NOP and placebo premixes were obtained weekly by mixing corn

grain (65%), soybean oil (5%), and either Bovaer10 or a placebo (10%). The delivered diets were obtained by mixing the basal diets with the premix corresponding to their respective treatment and were distributed using a self-moving mixer. During the 14-d washout period, no treatment was given, and all cows were fed the same diet.

Collection of Rumen Fluid and Milk Samples

At the end of the treatment period, rumen fluid was collected from all the enrolled cows immediately before feeding using an oro-esophageal ruminal probe specially designed for cattle (Ruminator; profs-products.com), as described by (Wallace et al., 2019). After discarding the first 0.5 L of collected fluid to avoid salivary contamination, 0.5 L of fluid was retained. The probe was rinsed with tap water after each sampling. After collection, pH was immediately measured with a pH meter (GLP 21; Crison Instruments SA). Then, samples were gently mixed and immediately cooled in iced water for subsequent measurement of VFA, lactic acid, and ammonia, with results reported in Moschini et al. (2025). A further aliquot of 1.5 mL per cow, without any additive, was transferred in 1.5-mL Eppendorf Safe-Lock Tubes, immediately frozen in dry ice, and then stored at −20°C until metabolite extraction, as will be described.

Cows were milked twice daily at 0400 and 1600 h. Individual milk samples (300 mL) were collected at the morning milking at the end of the treatment period, and a 15-mL aliquot was frozen at −20°C until metabolite extraction.

Extraction of Rumen and Milk Metabolites

Rumen metabolites were extracted using an ultrasound-assisted extraction method (Cattaneo et al., 2023). Briefly, samples were slowly thawed at 4°C, and 200 µL of rumen fluid was added to 800 µL of pre-cooled methanol/acetonitrile solution (1:1, vol/vol). The extraction step was promoted by an ultrasound-assisted extraction (DU-32 ARGOLab, Milan, Italy; power level: 120 W) at room temperature for 15 min. Thereafter, rumen samples were vortexed and centrifuged at 14,000 × *g* at 4°C for 20 min. The resulting supernatants were filtered through 0.22-µm cellulose syringe filters in ultra-HPLC vials until further untargeted metabolomic profiling. A total of 57 rumen samples were considered for the untargeted metabolomic analysis (Supplemental Table S1; see Notes).

The extraction of milk metabolites was carried out as previously reported by Rocchetti et al. (2022). The collected milk samples were skimmed by centrifugation at 4,500 × *g* for 10 min at 4°C. Thereafter, samples were thawed and thoroughly vortexed mixed. An aliquot of 2 mL was extracted with 14 mL of acetonitrile (liquid chromatography-MS grade, Sigma-Aldrich) added with 3% formic acid (vol/vol), mixed by vortexing for 2 min, and processed with ultrasound (DU-32 ARGOLab, Milan, Italy; power level: 120 W) for 5 min. Then, milk samples were centrifuged at 12,000 × *g* for 15 min at 4°C to remove large biomolecules (such as proteins). The supernatants were filtered through 0.22-µm cellulose syringe filters in ultra-HPLC vials until further untargeted metabolomic profiling. A total of 55 milk samples were considered for the untargeted metabolomic analysis (Supplemental Table S1), and 2 samples were excluded due to storage-related issues.

Untargeted Metabolomic Analysis

The untargeted analysis of milk and rumen samples, via ultra-HPLC coupled with high-resolution mass spectrometry, was conducted using a Q Exactive Focus Hybrid Quadrupole-Orbitrap Mass Spectrometer (Thermo Scientific, Waltham, MA) coupled to a Vanquish ultra-HPLC pump, equipped with a heated electrospray ionization (**HESI**)-II probe (Thermo Scientific). A detailed description of the instrumental conditions related to chromatography and mass spectrometry can be found in Cattaneo et al. (2023). Overall, chromatographic separation was achieved using an Acquity UPLC Waters BEH C18 column (2.1 × 100 mm, 1.7 µm), considering a gradient elution (6%–94% acetonitrile in 35 min) and 0.1% formic acid as phase modifier. The flow rate was 200 µL/min, injecting 6 µL of each sample. The untargeted analysis was performed in the full-scan range of 100 to 1,200, using a positive ionization mode and setting a mass resolution of 70,000. Additionally, a pooled quality control sample was randomly injected and analyzed in a data-dependent (top N ions = 3, under stepped normalized collisional energy) MS/MS mode, considering a full-scan mass resolution of 17,500. The HESI parameters, together with automatic gain control values and maximum injection times, are reported elsewhere (Rocchetti et al., 2022). The collected raw data were further processed using the software MS-DIAL (version 4.90; https://systemsomicslab.github.io/compms/msdial/main.html) for automatic peak detection, locally weighted scatterplot smoothing (LOWESS) normalization, and annotation via spectral matching against the comprehensive Bovine Metabolome Database (Foroutan et al., 2020). The identification step was based on mass accuracy, isotopic pattern, and spectral matching, thus reaching a level 2 of confidence in annotation (García-Pérez et al., 2024).

Multivariate Statistics and Pathway Analysis

Before multivariate analysis, rumen and milk metabolomics datasets were normalized by median, $\log_{10}$ transformed, and Pareto scaled (Rocchetti et al., 2022). Thereafter, data fusion analysis and interpretation were carried

out using the web-based platform OmicsAnalyst (Zhou et al., 2021). In particular, dimensionality reduction was performed using 2 different methods: unsupervised multiple co-inertia analysis (**MCIA**) and supervised data integration analysis for biomarker discovery using latent components (**DIABLO**). Also, to better understand relationships between key features of the 2 omics datasets, a correlation network was built considering DIABLO as the feature selection method (covariance parameter: 0.4) and Pearson as similarity matrix method (correlation threshold between-omics parameter: 0.5). The "rAMOPLS" package (version 0.2; Boccard and Rudaz, 2016; González-Ruiz et al., 2017) on RStudio (version 4.2.3; http://www.posit.co/) was then used for ANOVA multiblock orthogonal partial least squares analysis (**AMOPLS**), to check for the significance of treatment, phase, and their interaction on each omics dataset, evaluating several statistical parameters, such as goodness of fit (R^2Y), residual structure ratio (**RSR**), residual sum of squares (**RSS**), and their associated *P*-values (Becchi et al., 2024). The AMOPLS models were run on 57 rumen fluid samples and 55 milk samples. Missing values were processed by MS-DIAL, which replaces them with one-tenth of the minimum relative abundance detected for each metabolite. The software MetaboAnalyst 6.0 (Pang et al., 2024) was used to perform orthogonal projections to latent structures discriminant analysis (**OPLS-DA**), considering the pairwise comparison of 3-NOP versus CTR for both rumen fluid and milk metabolome datasets. The significant metabolites for prediction were extrapolated through a variable importance in projection (**VIP**) approach, considering also their $\log_2$ fold change (**FC**) variation. Finally, the online tool MetaboAnalyst 6.0 was used to inspect the changes of the most important pathways represented by the significant rumen metabolites annotated, using as pathway library *Bos taurus*, from the Kyoto Encyclopedia of Genes and Genomes (KEGG).

RESULTS AND DISCUSSION

Unsupervised and Supervised Discrimination of Rumen Fluid and Milk Metabolomes

In this study, the use of an untargeted metabolomics approach, combined with the Bovine Metabolome Database, enabled the putative annotation of 1,196 metabolites in rumen fluid and 846 metabolites in milk samples. Additionally, 191 (in rumen) and 140 metabolites (in milk) were structurally confirmed based on the tandem MS information provided by quality control samples (i.e., annotated by tandem MS). Overall, the enrichment classification tool of MetaboAnalyst 6.0 allowed us to group the metabolites detected, revealing in both biofluids a great abundance of AA and small peptides, followed by other compounds such as carbohydrates and conjugates, fatty acids and conjugates, nucleic acids (including purine, pyrimidines, and their derivatives), and feed-related compounds (such as metabolites of terpenoids and polyphenols). A detailed list reporting all the putatively annotated compounds (i.e., level 2 of confidence in identification and structural confirmation of the most abundant mass features) can be found in Supplemental Table S1.

To enhance the understanding of metabolomics findings, we used a data fusion approach to provide a dimension reduction analysis and to better understand the capability of both rumen and milk metabolites to explain the effects of each variability factor under investigation (i.e., treatment, phase, and their potential interaction). To this aim, the unsupervised MCIA and the supervised DIABLO approaches were carried out, and the results are presented in Figure 1A and Figure 1B, respectively. These methods identify components with high variance within datasets and strong cross-dataset correlation. The MCIA method captures shared variability, whereas DIABLO focuses on components that separate sample groups. The dimension reduction summary plots reported in Figure 1 allowed us to see how the top components were related to the individual omics data (from milk and rumen fluid) and to the metadata labels. The unsupervised MCIA approach (Figure 1A) showed a partial separation between groups on the first component, whereas components 2 through 5 showed almost complete overlap of the 4 experimental groups. Generally, the top 3 components of each omics layer captured 36.8% for milk and 31.3% for rumen fluid metabolome. Similarly, the supervised DIABLO approach confirmed a greater ability of component 1 to maximize group separation, suggesting greater discriminant weight of phase (P1 or P2) compared with treatment (3-NOP vs. CTR). As far as the variance explained by the DIABLO approach is concerned, the top 3 components of each omics layer captured a total of 35.6% for milk and 31.4% for rumen fluid metabolome, providing information similar to the results of the unsupervised and supervised dimensionality reduction approaches. Finally, a correlation network was used to identify both inter- and intra-omics correlations; the analysis revealed 1 subnetwork made by 37 nodes and 399 edges (Supplemental Table S1), indicating high correlation between the 2 omics datasets based on both rumen and milk metabolites.

The partial overlapping outlined by MCIA and DIABLO as a function of the 4 main groups hampered a proper understanding of the biological phenomenon. Therefore, as the next step, we used an AMOPLS approach to better investigate the discriminating effect and the possible interaction between treatment (3-NOP vs. CTR) and phase (P1 and P2). The discriminant model AMOPLS is able to simultaneously consider multiple response variables

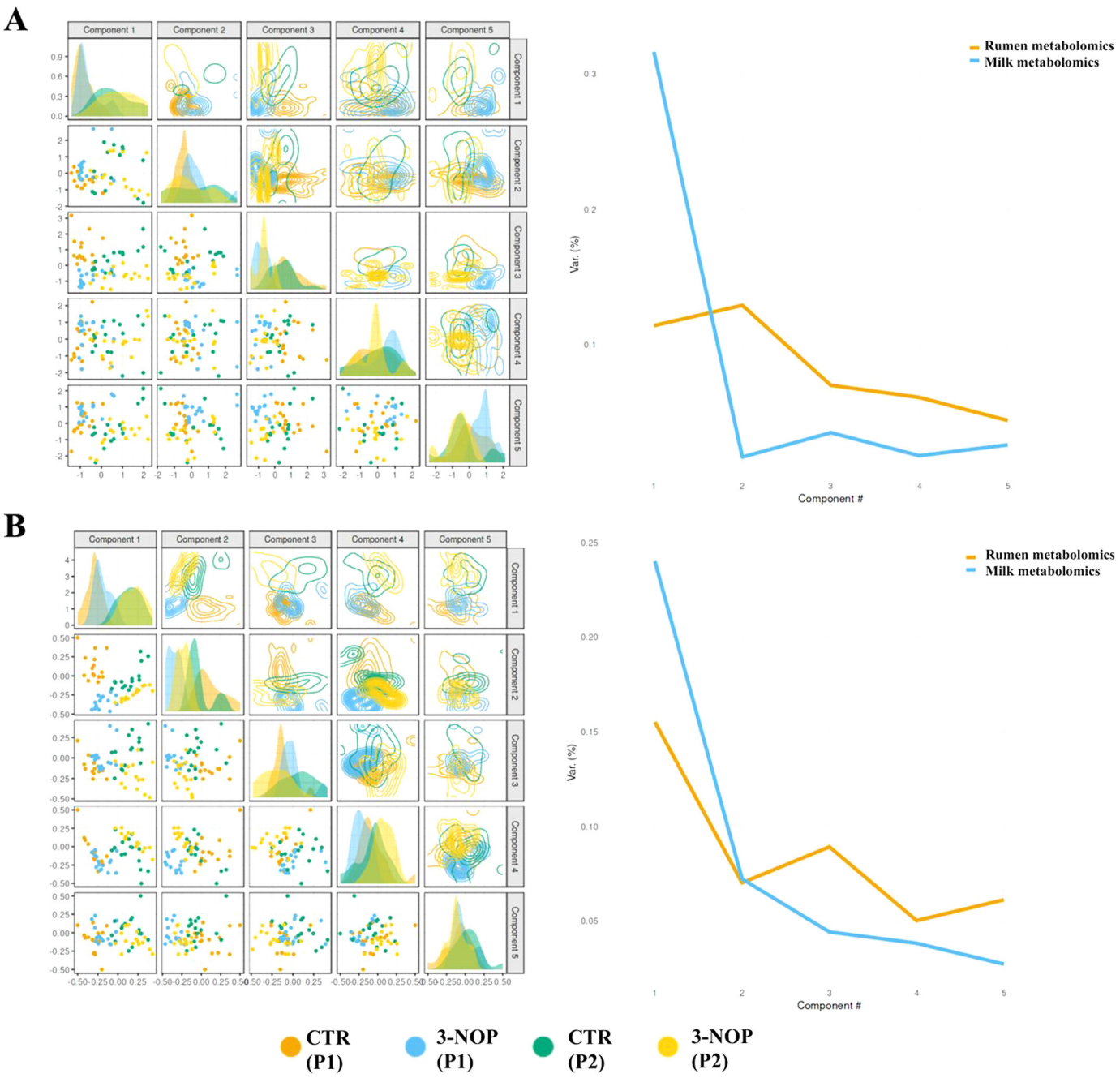

Figure 1. Multivariate integration of rumen and milk metabolomics datasets using 2 different multi-omics methods: (A) MCIA (multiple co-inertia analysis) and (B) DIABLO (Data Integration Analysis for Biomarker discovery using Latent variable approaches for Omics studies). Left panels (A and B): Pairwise scatterplots of the top 5 components derived from the integrated analyses. Each point represents an individual animal, color-coded by treatment group and study phase: CTR (P1) = control group in phase 1 of the study (orange); 3-NOP (P1) = group receiving 60 mg/kg DM of 3-nitrooxypropanol in phase 1 of the study (light blue); CTR (P2) = control group in phase 2 of the study (green); 3-NOP (P2) = group receiving 60 mg/kg DM of 3-nitrooxypropanol in phase 2 of the study (yellow). The diagonal shows the distribution (density plots) of individual component scores, and the off-diagonal panels show scatterplots and contour plots for each pair of components, allowing visualization of group clustering and separation across components. Right panels (A and B): Line plots representing the proportion of variance (Var.) explained by each of the top 5 components in each omics layer (rumen metabolome = orange line; milk metabolome = blue line), based on the integrated latent variables from MCIA or DIABLO. These plots highlight how each component contributes to capturing variation within each dataset.

Table 1. Relative variability and block contributions of the AMOPLS[1] analysis of rumen fluid and milk metabolome in lactating Holstein cows fed a diet supplemented with a placebo (control, CTR) or 3-NOP[2,3]

Item	RSS (%)	RSR	RSS *P*-value	RSR *P*-value	R^2Y *P*-value	tp1	tp2	tp3	to1
Rumen									
Treatment	5.0%	1.053	0.01	0.01	0.10	3.3%	82.8%	15.0%	25.5%
Phase	11.0%	1.254	0.01	0.01	0.01	89.9%	5.0%	12.6%	21.4%
Treatment × phase	2.4%	1.028	1.00	1.00	0.14	3.3%	6.0%	56.6%	26.2%
Residuals	81.6%	1.000	—	—	—	3.4%	6.2%	15.8%	26.9%
Milk									
Treatment	3.1%	1.028	0.01	0.08	0.03	1.3%	57.4%	13.4%	25.8%
Phase	9.3%	1.221	0.01	0.01	0.01	96.2%	12.4%	11.2%	21.7%
Treatment × phase	2.3%	1.016	1.00	1.00	0.09	1.3%	15.0%	61.7%	26.1%
Residuals	85.3%	1.000	—	—	—	1.3%	15.2%	13.7%	26.5%

[1]AMOPLS = ANOVA multi-block orthogonal partial least squares. The analysis was carried out considering the effects of treatment (CTR vs. 3-NOP), phase of the study, and their interaction.

[2]Dose of 3-NOP: 60 mg/kg DM.

[3]RSS = residual sum of squares; RSR = residual structure ratio; R^2Y = goodness of fit; tp = contribution of each main predictive component (1–3) used to build the score plot; to1 = contribution of orthogonal component.

(Becchi et al., 2024). This is particularly advantageous when dealing with multidimensional datasets, as it considers the eventual interactions among the response variables, leading to a more comprehensive and deeper understanding of the biological meaning. The statistical parameters associated with each effect are summarized in Table 1 for both milk and rumen metabolomic datasets. The results reveal that both treatment and phase (but not their interaction) are statistically significant and discriminant factors for the rumen fluid dataset (RSR *P*-values = 0.01), with phase showing the highest contribution to the model (RSS values 11% vs. 5%), as well as the highest RSR value (1.254). This effect was also evident by inspecting the high contribution of the first principal predictive component (**tp1** = 89.9%), associated with a low contribution of the orthogonal component (**to1** = 21.4%). In contrast, the interaction of treatment × phase did not show statistical significance, recording a lower RSS value (2.4%), and the residuals accounted for the remaining 81.6% of the total observed variability, indicating the presence of other sources of variation within the rumen fluid dataset. Regarding the milk metabolomic profile, the results revealed that only phase was statistically significant (RSR *P*-value = 0.01; RSS value: 9.3%), whereas treatment showed an RSR *P*-value >0.05 (*P* = 0.08), indicating a nonsignificant influence of 3-NOP on milk metabolome (Table 1). The greater significance of phase was also confirmed by inspecting the first principal predictive component (tp1), recording a value >96%, associated with a low contribution of the orthogonal component (to1 = 21.7%). As for the rumen, AMOPLS showed that the milk metabolomics dataset could not explain a high percentage of the total remaining variability (85.3%). Taken together, our findings revealed overlapping metabolomics profiles when comparing rumen fluid and milk metabolomes, suggesting a hierarchically higher effect of P1 and P2; accordingly, 3-NOP was found to mainly affect the rumen fluid metabolome, whereas AMOPLS outlined no significant differences in the milk metabolomics profiles.

The results obtained by the application of a data fusion approach on rumen and milk biofluids are coherent with the role exerted by 3-NOP as a methanogenesis inhibitor (Pitta et al., 2022a,b; Moschini et al., 2025). In this regard, microbes (such as bacteria, protozoa, fungi, and archaea) inhabit the rumen and work synergistically, digesting what is indigestible feed for the host. Methane is a natural by-product formed by methanogens (archaea) utilizing hydrogen (H_2), carbon dioxide (CO_2), methanol, and methylamines released primarily during carbohydrate and protein fermentation by other microbes (Buan, 2018; Pitta et al., 2022b).

Influence of 3-NOP on Rumen Metabolome and Evaluation of Enriched Pathways

To the best of our knowledge, no scientific works are available evaluating rumen fluid metabolome following the administration of 3-NOP as a methanogenesis inhibitor in lactating cows. Our companion paper (Moschini et al., 2025) demonstrated that 3-NOP significantly reduced enteric CH_4 production and yield by 46% while maintaining milk production and composition, animal health and welfare, and feed efficiency. Similarly, some previous works (Hristov et al., 2015; Melgar et al., 2020; Yanibada et al., 2021) have shown reduction of enteric CH_4 emissions between 23% and 30% with 3-NOP supplementation. The greater reduction observed in our study may be attributable to the diet, which was richer in corn silage and starch than the diets used in these previous studies.

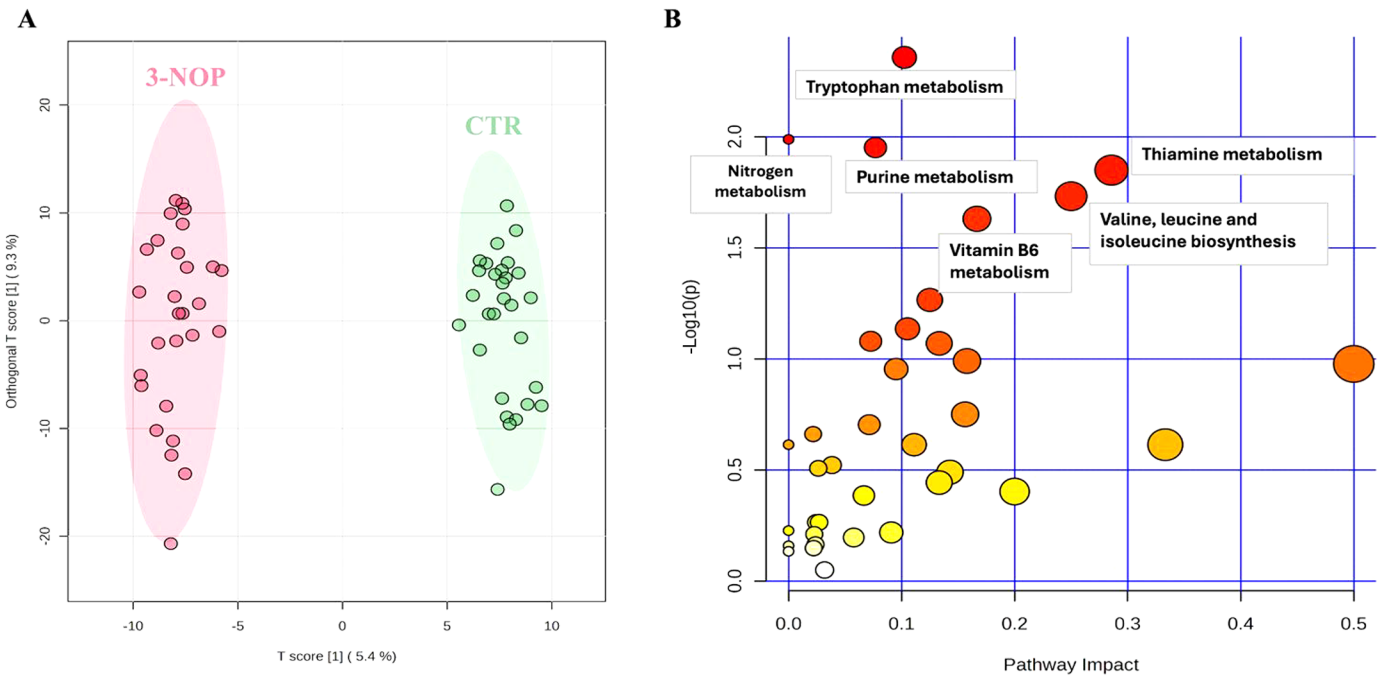

Figure 2. (A) Supervised orthogonal projections to latent structures discriminant analysis (OPLS-DA) score plot comparing the ruminal metabolomic profiles in lactating Holstein cows fed a diet supplemented with a placebo (CTR, green) or 3-NOP (pink). Each point represents an individual rumen fluid sample, with clear separation between the 2 groups along the first predictive component (T score [1]), indicating distinct metabolic profiles. (B) Pathway enrichment and topology analysis based on VIP (variable importance in projection) discriminant metabolites from the OPLS-DA model, mapped against *Bos taurus* metabolic pathways. The x-axis ("Pathway Impact") reflects the topological importance of each pathway, and the y-axis ($-Log_{10}(P)$) indicates the statistical significance of pathway enrichment. Circle color represents the *P*-value (from low significance [yellow] to high significance [red]), and circle size reflects the pathway impact value (larger size = higher impact on the overall metabolism). Key metabolic pathways significantly altered by 3-NOP treatment include tryptophan metabolism, purine metabolism, vitamin B_6 metabolism, thiamine metabolism, and branched-chain amino acid biosynthesis (valine, leucine, and isoleucine).

Therefore, starting from this evidence, we used a supervised statistical approach based on OPLS-DA and pathway analysis to better understand the fluctuations of rumen fluid metabolome when comparing 3-NOP versus CTR groups. The results of this supervised approach are graphically represented by the OPLS-DA score plot in Figure 2A and the pathway analysis plot against the metabolome of *Bos taurus* in Figure 2B. The OPLS-DA score plot provided clear discrimination between groups. However, it was characterized by a non-negotiable within-group variability (considering the importance of feeding phase as outlined by AMO-PLS). The OPLS-DA model was characterized by high goodness-related parameters, with goodness of fit (R^2Y) = 84.2% and goodness of prediction (Q^2) = 71.6%. As the next step, we extrapolated the most discriminant rumen metabolites for prediction using a VIP approach, with a minimum cutoff value of a score higher than 1. Among the discriminant metabolites (Table 2) we found 61 compounds included in the group of AA and small peptides, followed by 58 lipids and derivatives (including 26 fatty acyls, 9 glycerolipids, 18 glycerophospholipids, and 5 sphingolipids), 13 phenolic metabolites, 9 polyamines, 8 purines and derivatives, 5 pyrimidines and derivatives, 8 terpenoids, 3 medium-chain aldehydes, 7 indoles and derivatives, 3 pteridines, and 52 other compounds (including organooxygen compounds, organonitrogen compounds, benzenoids, carbohydrates and derivatives, organosulfonic acids, pyridines, quinolines, and steroids). The FC analysis showed that 3-NOP determined a significant up-accumulation of rumen AA and small peptides, followed by glycerophospholipids, sphingolipids, purines, pyrimidines, polyamines, medium-chain aldehydes, pteridines, and the remaining compounds classified as other metabolites. All the other classified chemical classes showed a cumulative down-accumulation, with fatty acyls and glycerolipids being the most affected chemical classes (Table 2).

Among the discriminant metabolites, we found a significantly high discriminating ability for some compounds, such as galactonic acid (area under the curve [**AUC**]: 0.97), N1-acetylspermidine (AUC: 0.97), capryloylglycine (AUC: 0.93), and octanol (AUC: 0.91). Galactonic acid is a derivative of galactose, one of the monosaccharides found in lactose and also in pectin galacturonic acid, and other carbohydrates present

Table 2. Chemical classes characterizing the different rumen fluid sample metabolomes in lactating Holstein cows fed a diet supplemented with a placebo (control, CTR) or 3-NOP[1]

Chemical class	Number of VIP[2] discriminant compounds	Log_2 fold change,[3] 3-NOP vs. CTR	Most discriminant VIP compound (OPLS-DA)[4]
Amino acids, peptides, and analogs	61	8.54	Capryloylglycine (VIP score: 2.38; AUC: 0.93; $P < 0.01$)
Fatty acyls and derivatives	26	−4.17	Octanol (VIP score: 2.53; AUC: 0.91; $P < 0.01$)
Glycerolipids	9	−1.84	MG(0:0/20:2(11Z,14Z)/0:0) (VIP score: 2.23; AUC: 0.90; $P < 0.01$)
Glycerophospholipids	18	7.25	PE(15:0/P-16:0) (VIP score: 1.96; AUC: 0.86; $P < 0.01$)
Sphingolipids	5	1.41	SM(d18:1/16:1(9Z)(OH)) (VIP score: 1.68; AUC: 0.78; $P < 0.01$)
Phenolic compounds	13	−1.59	Resveratrol (VIP score: 1.88; AUC: 0.84; $P < 0.01$)
Terpenoids	8	−1.11	4α-Formyl-4-methylzymosterol (VIP score: 1.63; AUC: 0.75; $P < 0.01$)
Purines and derivatives	8	8.91	8-Hydroxy-7-methylguanine (VIP score: 2.22; AUC: 0.83; $P < 0.01$)
Pyrimidines and derivatives	5	1.31	Dihydrothymine (VIP score: 1.20; AUC: 0.66; $P < 0.01$)
Polyamines	9	1.07	N1-Acetylspermidine (VIP score: 2.66; AUC: 0.97; $P < 0.01$)
Medium-chain aldehydes	3	2.78	4-Hydroxynonenal (VIP score: 1.82; AUC: 0.79; $P < 0.01$)
Indoles and derivatives	7	−1.05	Indolelactic acid (VIP score: 1.36; AUC: 0.73; $P < 0.01$)
Pteridines	3	0.66	6-Hydroxymethyl-7,8-dihydropterin (VIP score: 1.69; AUC: 0.78; $P < 0.01$)
Other metabolites	52	2.13	Galactonic acid (VIP score: 2.82; AUC: 0.97; $P < 0.01$)

[1]Dose of 3-NOP: 60 mg/kg DM.

[2]VIP = variable importance in projection.

[3]Cumulative log_2 fold change values for the pairwise comparison 3-NOP vs CTR.

[4]OPLS-DA = orthogonal projections to latent structures discriminant analysis; AUC = area under the curve; MG = monoacylglycerol; PE = phosphatidylethanolamine; SM = sphingomyelin; OH = hydroxyl group; Z = cis-configuration of the double bond.

in plants. Galactonic acid is an aldonic acid, specifically the oxidized form of galactose, where the aldehyde group is converted to a carboxylic acid group. Under our experimental conditions, galactonic acid was significantly down-accumulated in the 3-NOP group (log_2 FC = −3.15) compared with the CTR group, suggesting greater utilization of this compound, likely derived from pectin galacturonic acid, by the rumen microbiota as a fermentation substrate and carbon source. The lower levels of galactonic acid observed in cows fed with 3-NOP could indicate a shift in carbohydrate fermentation pathways. This trend may be due to changes in the ruminal microbiota composition, an increased microbial utilization of galactonic acid, or a modification in the metabolic fluxes linked to hydrogen balance and VFA production. Interestingly, Zhang et al. (2021) found a positive association between galactonic acid and *Christensenellaceae* in yaks, and Wang et al. (2023) reported a higher presence of *Firmicutes*, including *Christensenellaceae*, in goats with elevated ruminal propionate and butyrate levels, which is consistent with our results. These hypotheses reflect the complex ruminal microbiota–host interaction and its effect on nutrient metabolism (Liu et al., 2021). Further studies on microbial populations and metabolic fluxes could help clarify this trend.

The second highly discriminant compound was N1-acetylspermidine, a derivative of spermidine, a biogenic amine involved in various cellular processes, including cell growth, differentiation, and apoptosis (Kalač and Krausová, 2005). N1-Acetylspermidine is formed through the enzymatic acetylation of spermidine, a reaction typically catalyzed by spermidine/spermine N1-acetyltransferase (SSAT). This modification often serves as a regulatory mechanism to control polyamine levels within cells (Pegg, 2008). In this work, an overall down-accumulation of N1-acetylspermidine was outlined by FC analysis (log_2 FC = −1.98) in the 3-NOP group. At the same time, a concurring up-accumulation of other polyamines (such as spermidine) was found (Supplemental Table S1). Therefore, it can be suggested that 3-NOP administration may influence cooperative activities in the rumen microbiota through the action of polyamines, which are known to affect microbial interactions (Xi et al., 2023). Certain methanogenic bacteria can utilize

polyamines and their derivatives as nitrogen sources, influencing microbial growth and activity (Scherer and Kneifel, 1983; Xi et al., 2023).

The remaining highly discriminant metabolites, namely capryloylglycine and octanol, can be associated with the rumen modification of the medium-chain fatty acid octanoic acid (caprylic acid). In particular, capryloylglycine is a compound formed by combining octanoic acid and glycine (an amino acid). At the same time, octanol can be synthesized from octanoic acid through a hydrogenation process, which requires H_2. Looking at the FC analysis, capryloylglycine was down-accumulated in the 3-NOP group ($\log_2$ FC = −0.54), whereas an opposite trend was observed for octanol, recording an overall up-accumulation ($\log_2$ FC = 1.32). Additionally, the significant accumulation of medium-chain aldehydes, such as 4-hydroxynonenal (Table 2), a typical lipid peroxidation product, could be linked to the incomplete biohydrogenation of unsaturated fatty acids by rumen microbes. This may result from a microbial shift induced by 3-NOP and the accumulation of molecular hydrogen, potentially leading to the buildup of intermediate products prone to oxidation. This chemical behavior aligns with the intriguing hypothesis of a link between biohydrogenation and methanogenesis, as previously suggested in the scientific literature (Lourenço et al., 2010; Yang et al., 2019).

As far as the pathway analysis reported in Figure 2B, we found a significant ($P < 0.05$) enrichment of 6 different metabolic pathways involving the metabolism of AA (such as valine, leucine, and isoleucine), purines and pyrimidines, nitrogen (including glutamine and carbamoylphosphate), and vitamin B_6. An overall up-accumulation of isoleucine and leucine in the 3-NOP group was noted, with $\log_2$ FC values of 0.26 and 0.35, respectively. Generally, the up-accumulation of AA (Supplemental Table S1) and the significant enrichment of small peptides suggest that a higher microbial proteolytic activity characterized the 3-NOP group, or alternatively, there may be a delay or a disconnection in their utilization for the de novo synthesis of amino acids and microbial proteins. Proteolysis is a critical process in ruminant nutrition, and several factors are reported to critically influence the rate and extent of proteolysis by rumen microorganisms, including microbial composition, substrate characteristics, environmental conditions, and dietary factors (Bach et al., 2005). Therefore, we hypothesize that, by modulating the microbial composition in the rumen, 3-NOP may have influenced the proteolytic processes, not by increasing overall proteolysis but rather by promoting more efficient utilization of amino acids. This interpretation is supported by the observed reduction in both ruminal ammonia and plasma urea levels in the 3-NOP group compared with CTR, as also discussed by Moschini et al. (2025). Such evidence suggests a shift toward a more effective incorporation of nitrogen into microbial protein, rather than excessive amino acid deamination. Furthermore, the significant enrichment of metabolic pathways related to nucleic acid metabolism, together with the observed up-accumulation of purine and pyrimidine derivatives, is likely associated with increased nucleic acid biosynthesis and, consequently, greater microbial protein synthesis in the rumen (Rocchetti et al., 2022).

Finally, in the 3-NOP group, we observed significant up-accumulation of 4-pyridoxic acid, the final degradation product of vitamin B_6. This compound has been previously associated with changes in both the nutrient composition of diets and the structure of rumen microbial populations (Castagnino et al., 2016; Rocchetti et al., 2022). Although an increase in 4-pyridoxic acid could reflect enhanced vitamin B_6 catabolism, which might be interpreted as a negative outcome, it is also plausible that this observation results from a greater microbial production or turnover of vitamin B_6 in response to altered rumen microbial dynamics under 3-NOP supplementation. In this context, the accumulation of 4-pyridoxic acid may indicate a more active vitamin B_6 cycle, potentially supporting increased microbial metabolic activity. Nonetheless, further targeted studies are needed to elucidate whether the observed changes reflect improved vitamin B_6 availability and utilization or excessive degradation.

Going into the details of rumen methanogenesis, we used the untargeted metabolomics approach to inspect the relative abundance and prediction ability of some key metabolites involved in CH_4 formation. It is known from scientific literature (Pitta et al., 2022a) that despite the common end product, individual methanogens have distinct physiological and metabolic capabilities for survival, including substrate utilization, H_2 thresholds, responses to partial pressure of H_2, and structural differences in key enzymes, such as MCR and heterodisulfide reductase (HDR). The hydrogenotrophic pathway represents one of the main biochemical routes for CH_4 formation, where electrons are transferred along several one-carbon compounds before methyl-coenzyme M is formed (Pitta et al., 2022a). By inspecting the discriminant metabolites of the OPLS-DA prediction model (Figure 2A), we found 2 key metabolites, namely methyl-coenzyme M (belonging to organosulfonic acids) and coenzyme B (a coenzyme required for redox reactions in methanogens). Coherently with the observed lower enteric CH_4 emission and the inhibition of MCR by 3-NOP (Moschini et al., 2025), we found a significant down-accumulation of both methyl-coenzyme M and coenzyme B in the rumen of 3-NOP group, recording $\log_2$ FC values of −0.45 and −0.36, respectively (Supplemental Table S1). Interestingly, by inspecting the VIP discriminant metabolites, we found also a significant up-accumulation of 6-hydroxymethyl-7,8-

dihydropterin, a key intermediate belonging to the guanosine triphosphate (GTP) pathway, representing a potential alternative biochemical route to synthesize 5-methyltetrahydromethanopterin—that is, the precursor of methyl-coenzyme M (Pitta et al., 2022a). Additionally, the previously mentioned up-accumulation of octanol and the concurring down-accumulation of capryloylglycine is coherent with metabolization of the medium-chain fatty acid octanoic acid to process the excess of H_2 associated with inhibition of the hydrogenotrophic pathway.

Our in vivo findings agree with a recent work published by Luan et al. (2023), evaluating the effects of different dosages and types of medium-chain fatty acids (including octanoic, capric, and lauric acids) on rumen fermentation in vitro under low- and high-concentrate diets. The authors demonstrated that medium-chain fatty acids were all able to potentially reduce CH_4 production, and the number of rumen protozoa, methanogens, and *Methanobrevibacter* under the 2 diets with the dosages increased. Looking at some metagenomic works available in scientific literature, Pitta et al. (2022a) evaluated the effect of 3-NOP on ruminal microbial gene expression profiles in dairy cows. Interestingly, the authors revealed that 3-NOP was more inhibitory on *Methanobrevibacter* species than methanol-utilizing *Methanosphaera* and tended to reduce the gene expression of MCR. Under inhibited methanogenesis by 3-NOP, fluctuations in H_2 concentrations were accompanied by changes in the expression of [FeFe] hydrogenases in H_2-producing bacteria to regulate the amount of H_2 production, particularly increasing the synthesis of butyric acid as a compensatory mechanism. In this work, we have not measured a discriminant ability for butyric acid in the rumen (although a significant increase for this compound was reported in Moschini et al., 2025); however, a discriminant potential was found for some related metabolites, such as the fungal metabolite 4-guanidinobutanoic acid (log_2 FC: 0.93) and its oxidative product guanidinosuccinic acid (log_2 FC: 0.24). Nevertheless, the metagenomic findings from Pitta et al. (2022a) agree with our metabolomics results, clearly outlining the discriminant role of other biochemical pathways likely activated by an excess of H_2 production. Therefore, taken together, untargeted metabolomics confirmed the pivotal role exerted by rumen microorganisms, and future works based on the combination of different omics (such as metagenomics, metatranscriptomics, and metabolomics) seem to be of great interest to better understand the molecular basis of methanogenesis in the rumen and the interplay between key metabolites and microorganisms (Pitta et al., 2022a).

Changes in Milk Metabolome

Considering that the AMOPLS approach outlined a nonsignificant effect of 3-NOP, we used the supervised OPLS-DA modeling coupled with VIP, FC analysis, and receiver operating characteristic (**ROC**) curves to better maximize the between-group separation between 3-NOP and CTR groups. The most discriminant chemical classes and their log_2 FC accumulation values are graphically summarized in Figure 3. As a general consideration, we found that the most represented classes of milk metabolites consisted of fatty acyls and derivatives (19 compounds), followed by glycerophospholipids (18 compounds), AA and small peptides (17 compounds), glycerolipids (8 compounds), nucleic acids and derivatives (including both purines and pyrimidines, accounting for a total number of 12 compounds), steroids (8 compounds), polyamines (5 compounds), carbohydrates and conjugates (4 compounds), prenol lipids (mainly terpenoids), and phenolic metabolites.

Going into detail of the accumulation values (Supplemental Table S1), milk samples belonging to the 3-NOP group were mainly characterized by up-accumulation of glycerophospholipids (log_2 FC = 5.81), followed by AA and peptides (log_2 FC = 3.71), pyrimidines, and purines (log_2 FC values of 2.08 and 1.54, respectively). In contrast, the maximum down-accumulations were recorded for glycerolipids (log_2 FC = −3.68), fatty acyls (log_2 FC = −2.18), and polyamines (log_2 FC = −2.00). Regarding milk glycerophospholipids, we found a high abundance of lysophosphatidylcholines, with the compound LysoPC (20:0) outlined as the most discriminant (VIP score: 3.14) and significant (ROC AUC: 0.83), being clearly up-accumulated (log_2 FC: 0.74) in the 3-NOP group.

A previous work by Liu et al. (2017) investigated the importance of glycerophospholipids as heat stress biomarkers for dairy cattle. Interestingly, higher levels of polar lipids (such as lysophosphatidylcholines) have been observed in heat-tolerant cows compared with heat-susceptible ones during heat stress (Liu et al., 2017). In a previous work, Yanibada et al. (2021) used a multiplatform metabolomics approach to investigate changes in milk metabolic profiles related to methanogenesis in 25 primiparous Holstein dairy cows at similar lactation stages fed with the same antimethanogenic additive. Although working with a smaller sample size and evaluating few mass features, the authors found some milk metabolites likely originating from the rumen microbiota (or with a microbial–host animal co-metabolism) that could be associated with methanogenesis. Additionally, the other metabolic pathways significantly affected by 3-NOP were mainly associated with AA metabolism and fatty acids, corroborating our

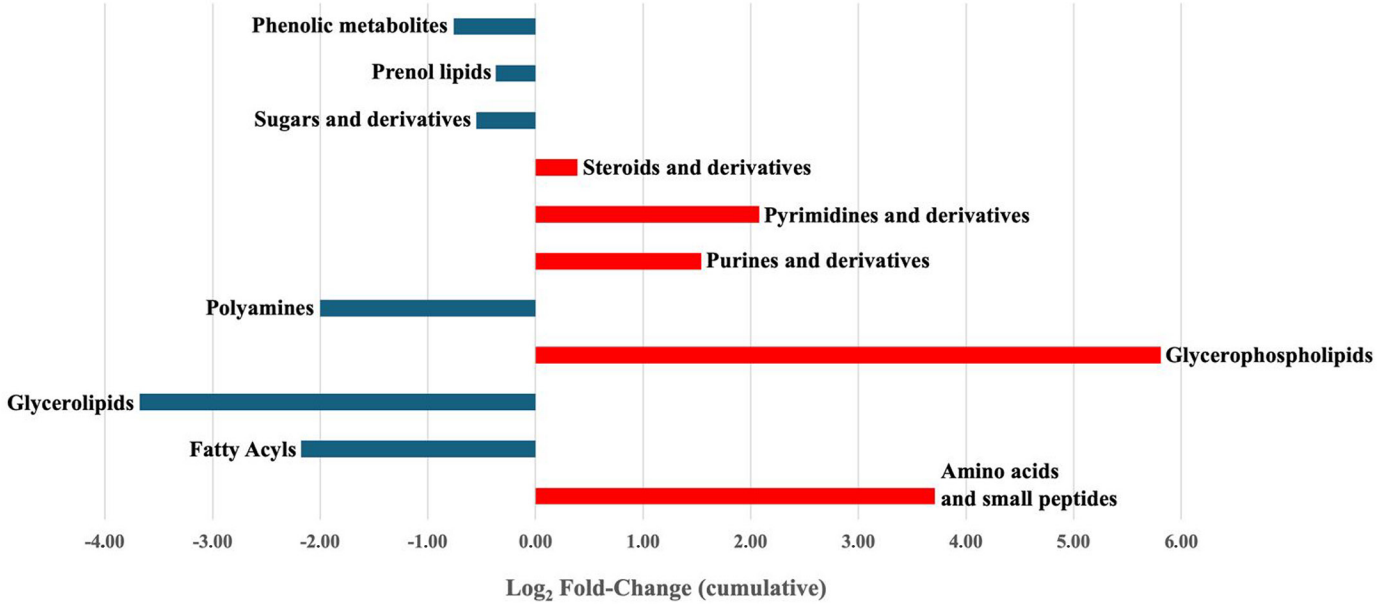

Figure 3. Accumulation values (expressed as $\log_2$ fold change) of the most discriminant chemical classes in milk samples for the pairwise comparison between lactating Holstein cows fed a diet supplemented with 3-NOP or a placebo. Red bar = up-accumulation in 3-NOP group; Blue bar = down-accumulation in 3-NOP group.

metabolomic findings. Also, the same authors (Yaniba-da et al., 2021) reported milk glycerophosphocholines among discriminant metabolites as a function of 3-NOP. These compounds are normal constituents in cow milk and have important functions in cellular metabolism associated with fatty acid oxidation and energy balance. However, there is limited research and understanding on how 3-NOP affects milk glycerophospholipids accumulation, highlighting the need for targeted studies.

Taking together, our findings suggest that the milk metabolome could reflect differences in enteric CH_4 emissions from lactating Holstein dairy cows. Particularly, the up-accumulation of nucleic acids in milk may be related to an increased total microbial N synthesis in the rumen (Rocchetti et al., 2022), and the concurring up-accumulation of glycerophospholipids and down-accumulation of polyamines (such as spermine) could be related to better ability of dairy cows to tolerate heat stress (which agrees with the only statistical significance of the phase factor, as resulting from the AMOPLS findings; Table 1). However, it is important to note that metabolite concentrations measured at a single time point do not capture dynamics of rumen pool sizes or passage rates, which are influenced by dry matter intake (which was lower in the first phase of the study) and liquid flow. Therefore, although inhibiting CH_4 production appears to have a potentially favorable effect on the milk chemical profile, these results should be interpreted with caution given the limitations of single time point sampling.

CONCLUSIONS

This work showed that rumen and milk metabolomes can reflect differences in enteric CH_4 emissions from lactating Holstein dairy cows. Using a data fusion approach, we identified several discriminant metabolites related to the effects of 3-NOP on rumen metabolome and up to 6 affected metabolic pathways, suggesting a pivotal role of rumen microorganisms in driving the observed chemical modifications. As far as milk composition is concerned, many of the discriminant metabolites that were found at greater concentrations in low-methane-emitting cows were general indicators of an unimpaired metabolic status (i.e., glycerophospholipids, small peptides, and nucleic acids). Therefore, based on the metabolomic findings, although the reduction in CH_4 production did not significantly alter the overall milk metabolome, 3-NOP appears to exert potentially favorable effects. At the same time, a hierarchically higher significance of 3-NOP was found in rumen fermentation and alternative biochemical routes. The results presented here support the use of untargeted metabolomics for biomarker discovery in dairy science.

NOTES

This study was partially funded by dsm-firmenich (Kaiseraugst, Switzerland). Research activities in the Department of Animal Science, Food and Nutrition of the Università Cattolica del Sacro Cuore are supported by the Romeo and Enrica Invernizzi Foundation (Mi-

lan, Italy). This work is part of the NODES project, which has received funding from the MUR – M4C2 1.5 of PNRR, which was funded by the European Union – NextGenerationEU (Grant agreement no. ECS00000036 – CUP B43D21010950006). Supplemental material for this article is available at https://doi.org/10.17632/jv6m689jvv.1. This study was approved by the Committee for the Protection and Welfare of Experimental Animals of the Università Cattolica del Sacro Cuore and authorized by the Italian Health Ministry (protocol 355/2022-PR). The authors have not stated any conflicts of interest.

Nonstandard abbreviations used: 3-NOP = 3-nitrooxypropanol; AMOPLS = ANOVA multi-block orthogonal partial least squares; AUC = area under the curve; CTR = control group; DIABLO = data integration analysis for biomarker discovery using latent components; FC = fold change; HESI = heated electrospray ionization; MCIA = multiple co-inertia analysis; MCR = methyl-coenzyme M reductase; OPLS-DA = orthogonal projections to latent structures discriminant analysis; P1 = study phase 1; P2 = study phase 2; ROC = receiver operating characteristic; RSR = residual structure ratio; RSS = residual sum of squares; to = contribution of orthogonal component; tp = contribution of each main predictive component; VIP = variable importance in projection.

REFERENCES

Bach, A., S. Calsamiglia, and M. D. Stern. 2005. Nitrogen metabolism in the rumen. J. Dairy Sci. 88:E9–E21. https://doi.org/10.3168/jds.S0022-0302(05)73133-7.

Beauchemin, K. A., E. M. Ungerfeld, R. J. Eckard, and M. Wang. 2020. Review: Fifty years of research on rumen methanogenesis: Lessons learned and future challenges for mitigation. Animal 14:s2–s16. https://doi.org/10.1017/S1751731119003100.

Becchi, P. P., G. Rocchetti, P. García-Pérez, S. Michelini, V. Pizzamiglio, and L. Lucini. 2024. Untargeted metabolomics and machine learning unveil quality and authenticity interactions in grated Parmigiano Reggiano PDO cheese. Food Chem. 447:138938. https://doi.org/10.1016/j.foodchem.2024.138938.

Becchi, P. P., G. Rocchetti, and L. Lucini. 2025. Advancing dairy science through integrated analytical approaches based on multi-omics and machine learning. Curr. Opin. Food Sci. 63:101289. https://doi.org/10.1016/j.cofs.2025.101289.

Boccard, J., and S. Rudaz. 2016. Exploring omics data from designed experiments using analysis of variance multiblock orthogonal partial least squares. Anal. Chim. Acta 920:18–28. https://doi.org/10.1016/j.aca.2016.03.042.

Buan, N. R. 2018. Methanogens: Pushing the boundaries of biology. Emerg. Top. Life Sci. 2:629–646. https://doi.org/10.1042/ETLS20180031.

Castagnino, D. S., M. Seck, V. Beaudet, K. L. Kammes, J. A. Voelker Linton, M. S. Allen, R. Gervais, P. Y. Chouinard, and C. L. Girard. 2016. Effects of forage family on apparent ruminal synthesis of B vitamins in lactating dairy cows. J. Dairy Sci. 99:1884–1894. https://doi.org/10.3168/jds.2015-10319.

Cattaneo, L., G. Rocchetti, F. Piccioli-Cappelli, S. Zini, E. Trevisi, and A. Minuti. 2023. Impact of dry-off and lyophilized *Aloe arborescens* supplementation on plasma metabolome of dairy cows. Sci. Rep. 13:5256. https://doi.org/10.1038/s41598-023-31922-z.

de Almeida, R. T. R., R. M. do Prado, C. Porto, G. T. dos Santos, S. A. Huws, and E. J. Pilau. 2018. Exploring the rumen fluid metabolome using liquid chromatography-high-resolution mass spectrometry and Molecular Networking. Sci. Rep. 8:17971. https://doi.org/10.1038/s41598-018-36196-4.

EFSA. 2021. Safety and efficacy of a feed additive consisting of 3-nitrooxypropanol (Bovaer 10) for ruminants for milk production and reproduction (DSM Nutritional Products Ltd.). Panel on Additives and Products or Substances used in Animal Feed (FEEDAP). EFSA J. 19:e06905. https://doi.org/10.2903/j.efsa.2021.6905.

Foroutan, A., C. Fitzsimmons, R. Mandal, H. Piri-Moghadam, J. Zheng, A. Guo, C. Li, L. L. Guan, and D. S. Wishart. 2020. The bovine metabolome. Metabolites 10:233. https://doi.org/10.3390/metabo10060233.

García-Pérez, P., P. P. Becchi, L. Zhang, G. Rocchetti, and L. Lucini. 2024. Metabolomics and chemometrics: The next-generation analytical toolkit for the evaluation of food quality and authenticity. Trends Food Sci. Technol. 147:104481. https://doi.org/10.1016/j.tifs.2024.104481.

González-Ruiz, V., J. Pezzatti, A. Roux, L. Stoppini, J. Boccard, and S. Rudaz. 2017. Unravelling the effects of multiple expermental factors in metabolomics, analysis of human cells with hydrophilic interaction liquid chromatography hyphenated to high resolution mass spectrometry. J. Chromatogr. A 1527:53–60. https://doi.org/10.1016/j.chroma.2017.10.055.

Hristov, A. N., J. Oh, F. Giallongo, T. W. Frederick, M. T. Harper, H. L. Weeks, A. F. Branco, P. J. Moate, M. H. Deighton, S. R. Williams, M. Kindermann, and S. Duval. 2015. An inhibitor persistently decreased enteric methane emission from dairy cows with no negative effect on milk production. Proc. Natl. Acad. Sci. USA 112:10663–10668. https://doi.org/10.1073/pnas.1504124112.

Kalač, P., and P. Krausová. 2005. A review of dietary polyamines: Formation, implications for growth and health and occurrence in foods. Food Chem. 90:219–230. https://doi.org/10.1016/j.foodchem.2004.03.044.

Kebreab, E., A. Bannink, E. M. Pressman, N. Walker, A. Karagiannis, S. van Gastelen, and J. Dijkstra. 2023. A meta-analysis of effects of 3-nitrooxypropanol on methane production, yield, and intensity in dairy cattle. J. Dairy Sci. 106:927–936. https://doi.org/10.3168/jds.2022-22211.

Khairunisa, B. H., C. Heryakusuma, K. Ike, B. Mukhopadhyay, and D. Susanti. 2023. Evolving understanding of rumen methanogen ecophysiology. Front. Microbiol. 14:1296008. https://doi.org/10.3389/fmicb.2023.1296008.

Króliczewska, B., E. Pecka-Kiełb, and J. Bujok. 2023. Strategies used to reduce methane emissions from ruminants: Controversies and issues. Agriculture 13:602. https://doi.org/10.3390/agriculture13030602.

Liu, K., Y. Zhang, Z. Yu, Q. Xu, N. Zheng, S. Zhao, G. Huang, and J. Wang. 2021. Ruminal microbiota-host interaction and its effect on nutrient metabolism. Anim. Nutr. 7:49–55. https://doi.org/10.1016/j.aninu.2020.12.001.

Liu, Z., V. Ezernieks, J. Wang, N. Wanni Arachchillage, J. B. Garner, W. J. Wales, B. G. Cocks, and S. Rochfort. 2017. Heat stress in dairy cattle alters lipid composition of milk. Sci. Rep. 7:961. https://doi.org/10.1038/s41598-017-01120-9.

Liu, Z., K. Wang, X. Nan, M. Cai, L. Yang, B. Xiong, and Y. Zhao. 2022. Synergistic effects of 3-nitrooxypropanol with fumarate in the regulation of propionate formation and methanogenesis in dairy cows in vitro. Appl. Environ. Microbiol. 88:e0190821. https://doi.org/10.1128/aem.01908-21.

Lourenço, M., E. Ramos-Morales, and R. J. Wallace. 2010. The role of microbes in rumen lipolysis and biohydrogenation and their manipulation. Animal 4:1008–1023. https://doi.org/10.1017/S175173111000042X.

Luan, J., X. Feng, D. Yang, M. Yang, J. Zhou, and C. Geng. 2023. Effects of medium-chain fatty acids (MCFAs) on in vitro rumen fermentation, methane production, and nutrient digestibility under low- and high-concentrate diets. Anim. Sci. J. 94:e13818. https://doi.org/10.1111/asj.13818.

Melgar, A., K. C. Welter, K. Nedelkov, C. M. M. R. Martins, M. T. Harper, J. Oh, S. E. Räisänen, X. Chen, S. F. Cueva, S. Duval, and A.

N. Hristov. 2020. Dose-response effect of 3-nitrooxypropanol on enteric methane emissions in dairy cows. J. Dairy Sci. 103:6145–6156. https://doi.org/10.3168/jds.2019-17840.

Min, B. R., S. Solaiman, H. M. Waldrip, D. Parker, R. W. Todd, and D. Brauer. 2020. Dietary mitigation of enteric methane emissions from ruminants: A review of plant tannin mitigation options. Anim. Nutr. 6:231–246. https://doi.org/10.1016/j.aninu.2020.05.002.

Moschini, M., F. Froldi, F. Piccioli-Cappelli, P. Bani, E. Fiorbelli, A. Gallo, I. Mueller, L. F. M. Tamassia, R. Zihlmann, P. Bulgarelli, S. Agazzi, E. Trevisi, and L. Cattaneo. 2025. Effects of 3-nitrooxypropanol on enteric methane emissions and milk production characteristics in dairy cows fed a high corn–silage diet in different environmental conditions. J. Dairy Sci. 108:13455–13473. https://doi.org/10.3168/jds.2025-26640.

Pang, Z., Y. Lu, G. Zhou, F. Hui, L. Xu, C. Viau, A. F. Spigelman, P. E. MacDonald, D. S. Wishart, S. Li, and J. Xia. 2024. MetaboAnalyst 6.0: Towards a unified platform for metabolomics data processing, analysis and interpretation. Nucleic Acids Res. 52(W1):W398–W406. https://doi.org/10.1093/nar/gkae253.

Pegg, A. E. 2008. Spermidine/spermine-N(1)-acetyltransferase: A key metabolic regulator. Am. J. Physiol. Endocrinol. Metab. 294:E995–E1010. https://doi.org/10.1152/ajpendo.90217.2008.

Pitta, D. W., N. Indugu, A. Melgar, A. Hristov, K. Challa, B. Vecchiarelli, M. Hennessy, K. Narayan, S. Duval, M. Kindermann, and N. Walker. 2022a. The effect of 3-nitrooxypropanol, a potent methane inhibitor, on ruminal microbial gene expression profiles in dairy cows. Microbiome 10:146. https://doi.org/10.1186/s40168-022-01341-9.

Pitta, D., N. Indugu, K. Narayan, and M. Hennessy. 2022b. *Symposium review:* Understanding the role of the rumen microbiome in enteric methane mitigation and productivity in dairy cows. J. Dairy Sci. 105:8569–8585. https://doi.org/10.3168/jds.2021-21466.

Rocchetti, G., F. Ghilardelli, E. Carboni, A. S. Atzori, F. Masoero, and A. Gallo. 2022. Milk metabolome reveals pyrimidine and its degradation products as the discriminant markers of different corn silage-based nutritional strategies. J. Dairy Sci. 105:8650–8663. https://doi.org/10.3168/jds.2022-21903.

Scherer, P., and H. Kneifel. 1983. Distribution of polyamines in methanogenic bacteria. J. Bacteriol. 154:1315–1322. https://doi.org/10.1128/jb.154.3.1315-1322.1983.

Suh, J. H. 2022. Critical review: Metabolomics in dairy science—Evaluation of milk and milk product quality. Food Res. Int. 154:110984. https://doi.org/10.1016/j.foodres.2022.110984.

Toral, P. G., L. Abecia, G. Hervás, D. R. Yánez-Ruiz, and P. Frutos. 2023. Plasma and milk metabolomics in lactating sheep divergent for feed efficiency. J. Dairy Sci. 106:3947–3960. https://doi.org/10.3168/jds.2022-22609.

Wallace, R. J., G. Sasson, P. C. Garnsworthy, I. Tapio, E. Gregson, P. Bani, P. Huhtanen, A. R. Bayat, F. Strozzi, F. Biscarini, T. J. Snelling, N. Saunders, S. L. Potterton, J. Craigon, A. Minuti, E. Trevisi, M. L. Callegari, F. P. Cappelli, E. H. Cabezas-Garcia, J. Vilkki, C. Pinares-Patino, K. O. Fliegerová, J. Mrázek, H. Sechovcová, J. Kopečný, A. Bonin, F. Boyer, P. Taberlet, F. Kokou, E. Halperin, J. L. Williams, K. J. Shingfield, and I. Mizrahi. 2019. A heritable subset of the core rumen microbiome dictates dairy cow productivity and emissions. Sci. Adv. 5:eaav8391. https://doi.org/10.1126/sciadv.aav8391.

Wang, D., G. Tang, Y. Wang, J. Yu, L. Chen, J. Chen, Y. Wu, Y. Zhang, Y. Cao, and J. Yao. 2023. Rumen bacterial cluster identification and its influence on rumen metabolites and growth performance of young goats. Anim. Nutr. 15:34–44. https://doi.org/10.1016/j.aninu.2023.05.013.

Xi, H., X. Nie, F. Gao, X. Liang, H. Li, H. Zhou, U. Cai, and C. Yang. 2023. A bacterial spermidine biosynthetic pathway via carboxyaminopropylagmatine. Sci. Adv. 9:eadj9075. https://doi.org/10.1126/sciadv.adj9075.

Yang, C., N. McKain, C. A. McCartney, and R. J. Wallace. 2019. Consequences of inhibiting methanogenesis on the biohydrogenation of fatty acids in bovine ruminal digesta. Anim. Feed Sci. Technol. 254:114189. https://doi.org/10.1016/j.anifeedsci.2019.05.012.

Yanibada, B., U. Hohenester, M. Pétéra, C. Canlet, S. Durand, F. Jourdan, J. Boccard, C. Martin, M. Eugène, D. P. Morgavi, and H. Boudra. 2020. Inhibition of enteric methanogenesis in dairy cows induces changes in plasma metabolome highlighting metabolic shifts and potential markers of emission. Sci. Rep. 10:15591. https://doi.org/10.1038/s41598-020-72145-w.

Yanibada, B., U. Hohenester, M. Pétéra, C. Canlet, S. Durand, F. Jourdan, A. Ferlay, D. P. Morgavi, and H. Boudra. 2021. Milk metabolome reveals variations on enteric methane emissions from dairy cows fed a specific inhibitor of the methanogenesis pathway. J. Dairy Sci. 104:12553–12566. https://doi.org/10.3168/jds.2021-20477.

Yu, G., K. A. Beauchemin, and R. Dong. 2021. A review of 3-nitrooxypropanol for enteric methane mitigation from ruminant livestock. Animals (Basel) 11:3540. https://doi.org/10.3390/ani11123540.

Zhang, X., T. Xu, X. Wang, Y. Geng, N. Zhao, L. Hu, H. Liu, S. Kang, and S. Xu. 2021. Effect of dietary protein levels on dynamic changes and interactions of ruminal microbiota and metabolites in yaks on the Qinghai-Tibetan plateau. Front. Microbiol. 12:684340. https://doi.org/10.3389/fmicb.2021.684340.

Zhou, G., J. Ewald, and J. Xia. 2021. OmicsAnalyst: A comprehensive web-based platform for visual analytics of multi-omics data. Nucleic Acids Res. 49(W1):W476–W482. https://doi.org/10.1093/nar/gkab394.

ORCIDS

G. Rocchetti, https://orcid.org/0000-0003-3488-4513
F. Froldi, https://orcid.org/0009-0001-8157-9602
M. Lapris, https://orcid.org/0009-0007-0135-1178
M. Moschini, https://orcid.org/0000-0002-7167-709X
P. Bani, https://orcid.org/0000-0002-5334-1015
L. Cattaneo, https://orcid.org/0000-0001-6027-7536
E. Trevisi https://orcid.org/0000-0003-1644-1911